REPORT CAM PROJECT

Group 54

Andrea Ricciardi 10931392

Marino Carlone 10696425

Sebastiano Calefato 10935491

Contents

1) Notation and Formulas

D_c	Cutter Diameter	[mm]
Z	Number of cutting edges	-
v_c	Cutting speed	[m/min]
n	Rotational speed	[rpm]
$\omega = 2\pi \frac{n}{60}$	Angular speed	[rad/s]
f	Cutting feed	[mm/rev]
$f_Z = \frac{f}{Z}$	Feed per tooth	[mm/rev]
$v_f = Z \cdot f_Z \cdot n$	Feed Velocity	[m/min]
h_D	Chip thickness	[mm/rev]
A_D	Chip section area	[mm^2/rev]
f_Z	Feed per tooth	[mm/rev/tooth]
P_c	Cutting Power	[W]
k_{cs}	Specific Cutting Pressure	[MPa]
x	Kronenberg coefficient	-
a_e	Radial depth of Cut	[mm]
a_p	Axial depth of Cut	[mm]
k_r	Primary entering angle	[deg]
$k_r^{'}$	Secondary entering angle	[deg]
r	Cutting edge radius	[mm]
θ	Point angle	[deg]
z	Working teeth	-

Milling formulas

$$z = \frac{\varphi}{\varphi_0} \qquad \varphi_0 = \frac{2\pi}{Z}$$

$$F_c(\vartheta) = k_{c,\vartheta} \cdot A_{D,\vartheta}$$

$$T_c = \sum_{i=1}^{z} F_c(\vartheta) \frac{D/2}{1000}$$

$$P_c = T_c \cdot \omega$$

$$h_{D,av} = \frac{f_Z}{\varphi} \frac{2a_e}{D}$$

Face milling

$$h_{D,\vartheta} = f_z cos(\vartheta) sin(k_r)$$

$$A_{D,\vartheta} = h_D \frac{a_p}{sin(k_r)} = f_z cos(\vartheta) a_p$$

$$R_a = \frac{f^2}{32r} \cdot 10^3 [\mu m]$$

Slab milling

$$h_{D,\vartheta} = f_z sin(\vartheta)$$

$$A_{D,\vartheta} = h_D \cdot a_p$$

Drilling formulas

$$h_D = f_Z sin(\frac{\theta}{2})$$

$$A_D = f_Z \cdot \frac{D}{2}$$

$$F_c = k_c \cdot A_D$$

$$T_c = F_c \frac{D/2}{1000}$$

$$P_c = T_c \cdot \omega$$

Reaming/Counterboring formulas

$$h_D = f_Z$$

$$A_D = f_Z \frac{D_{ext} - D_{int}}{2}$$

$$F_c = k_c \cdot A_D$$

$$T_c = Z \cdot F_c \cdot \frac{\frac{D_{ext}/2 + D_{int}/2}{2}}{1000}$$

$$P_c = T_c \cdot \omega$$

2) Introduction

The project consists of modeling the final product in CAD software given the 2D technical drawing and performing machining operations on a rectangular stock to get the final product.

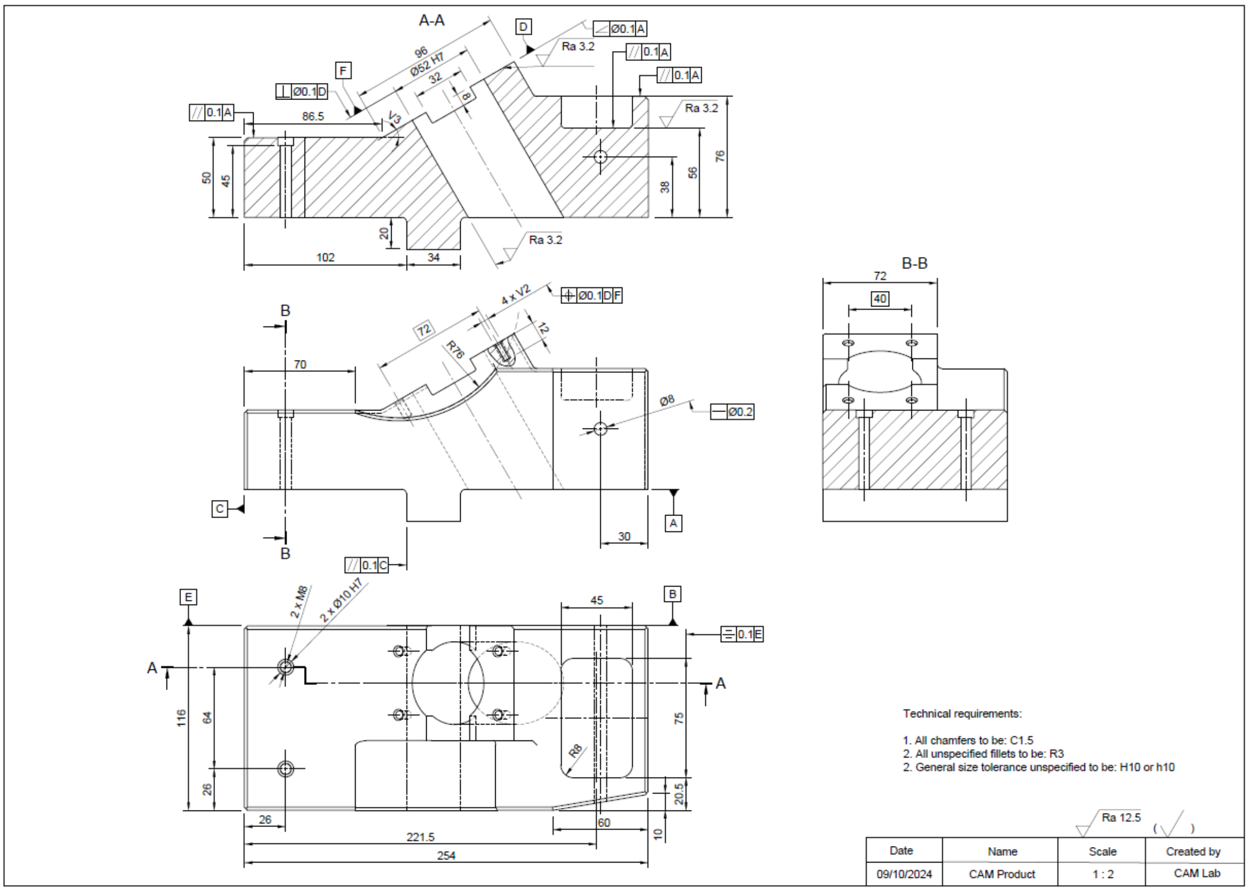

Information of the machine tool		
Attributes	Unit	Parameters
Working Area (X, Y, Z)	mm	1160 x 1000 x 900
Rapid Speed	m/min	42
Maximum Spindle Rotational Speed	rpm	14000
Spindle Power	kW	16
Spindle Repositioning Time	s	5
Tool Changing Time	s	15
Loading and Unloading Time	s	60

2.1 Inputs and Variables

Variables		
Name	No.	Value
Workpiece Material	V1	P1.4.Z.AN
Threaded Holes	V2	M7 x 1
Tilted Angle [°]	V3	30
Stock Size (xyz) [mm]	V4	260x122x128

Workpiece Material:

MC code	Material group		Material sub-group		Manufacturing process		Heat treatment		nom	Specific cutting force, k_{c1} (N/mm^2)	m_c
P1.1.Z.AN	1	unalloyed Mn<1.65	1	<=0.25% C	Z	forged/rolled/cold drawn	AN	annealed	125 HB	1500	0.25
P1.1.Z.HT	1		1		Z		HT	hardened+tempered	190 HB	1770	0.25
P1.2.Z.AN	1		2	>0.25... <=0.55% C	Z	forged/rolled/cold drawn	AN	annealed	190 HB	1700	0.25
P1.2.Z.HT	1		2		Z		HT	hardened+tempered	210 HB	1820	0.25
P1.3.Z.AN	1		3	high carbon, >0.55% C	Z	forged/rolled/cold drawn	AN	annealed	190 HB	1750	0.25
P1.3.Z.HT	1		3		Z		HT	hardened+tempered	300 HB	2000	0.25
P1.4.Z.AN	1		4	free cutting steel	Z	forged/rolled/cold drawn	AN	annealed	220 HB	1180	0.25

Threaded Holes:

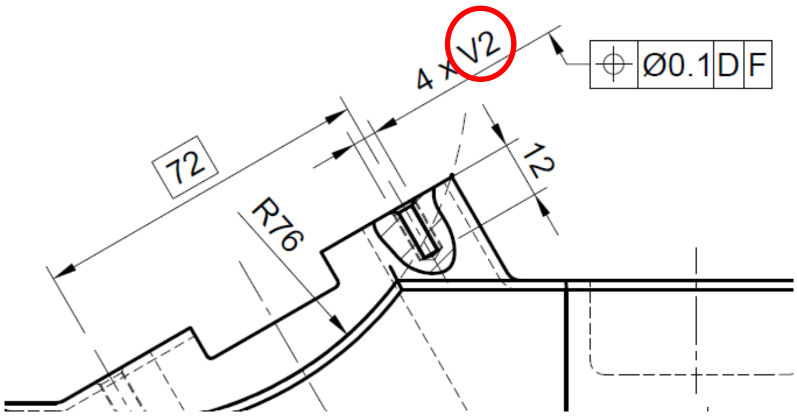

Tilted Angle:

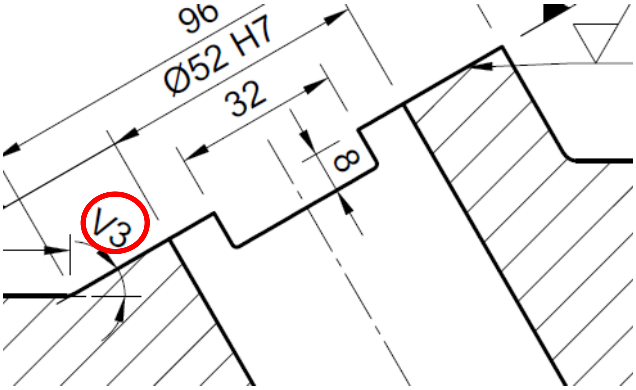

Stock Size:

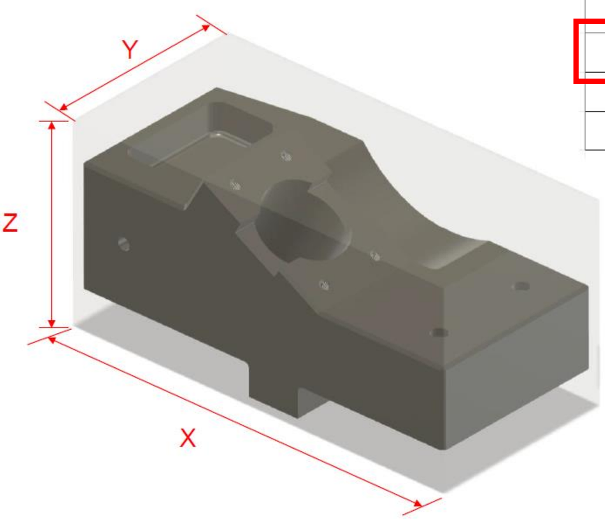

Stock size (mm)	X	Y	Z
1	260	122	128
2	262	124	130
3	264	126	132

2.2 Features and Operations

	Features
Top Surface	Pocket
	Curved Surface
	2 Counterbore Thread Holes
	Chamfers
	Fillets
Top Tilted Surface	Large Through Hole
	4 Countersink Blind Thread Holes
	2 Slots
	Fillets
Lateral Surface	Deep Through Hole
	Shifted Surface
	Chamfers
Bottom Surface	Fillets

We divided the operations into **5 setups:**

LEFT-L, **RIGHT-R**, **BOTTOM-B**, **TOP-U** and **FRONT-BACK-FB**:

NUMBER	CODE	NAME	OPERATION	TOOL #
1	L1	Left Surface	Face Milling	T1
2	R1	Right Surface 1	Slab Milling	T2
3	R2	Right Surface 2	Slab Milling	T2
4	R3	Curved Surface	Slab Milling	T2
5	R4	Drilling Deep Through Hole	Drilling	T3
6	B1	Bottom Surface	Pocketing	T4
7	B2	Bottom Fillets	Filleting	T5
8	U1	Top Surface	Pocketing	T2
9	U2	Top Tilted Surface Roughing	Pocketing	T2
10	U3	Slots	Pocketing	T2
11	U4	Right Surface Tilted Face	Pocketing	T2
12	U5	Pocket Roughing	Pocketing	T2
13	U6	Large Through Hole Roughing	Drilling	T6
14	U7	Pre-Drilling Blind Holes	Drilling	T7
15	U8	Pre-Drilling Through Holes	Drilling	T8
16	U9	Counterbore Roughing	Drilling	T9
17	U10	Top Tilted Surface Finishing	Face Milling	T10
18	U11	Pocket Finishing	Pocketing	T10
19	U12	Large Through Hole Finishing	Boring	T11
20	U13	Counterbore Reaming	Reaming	T15
21	U14	Countersinking Blind Holes	Countersinking	T12
22	U15	Tapping Blind Holes	Tapping	T13
23	U16	Tapping Through Holes	Tapping	T14
24	U17	Top Surface and Pocket Fillets	Filleting	T5
25	U18	Slots Fillets	Filleting	T5
26	FB1	Front Surface	Slab Milling	T2
27	FB2	Back Surface	Slab Milling	T2
28	FB3	Back Surface Corner Chamfers	Slab Milling	T2
29	FB4	Left Surface Chamfers	Chamfering	T16

30	FB5	Left Tilted Surface Chamfers	Chamfering	T16
31	FB6	Right Surface Chamfers	Chamfering	T16
32	FB7	Right Curved Surface Chamfers	Chamfering	T16
33	FB8	Top Surface Chamfers	Chamfering	T16

2.3 Precedence Graph

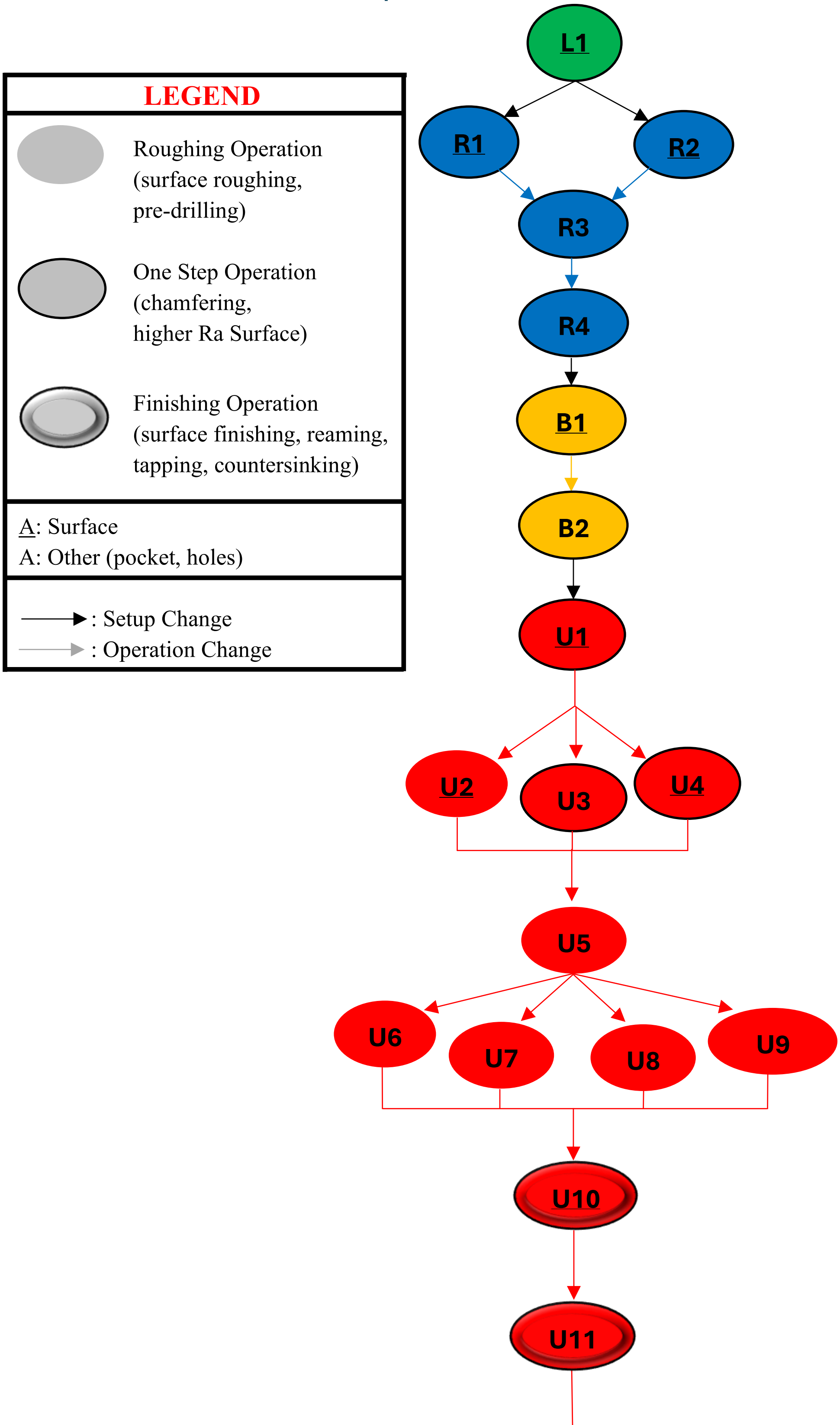

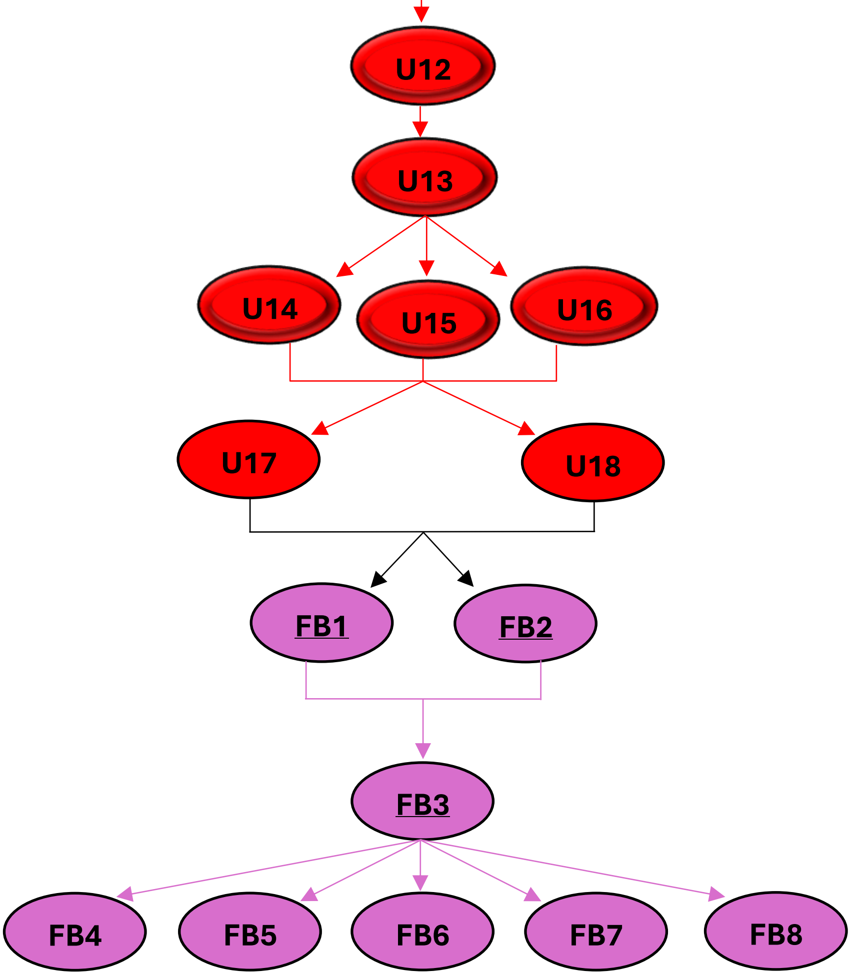

The operations that we carried out follow these 2 rules:

1. First **ROUGHING** and then **FINISHING** operations
2. First **SURFACE** and then **HOLE/POCKET**

This is done to have better references to create holes and pockets and to avoid the finished surface getting ruined by other rough operations.

3) Detailed Final Solution

This section provides a detailed explanation of how we realized the machining operations to obtain the final product in detail.

3.1 Throughput

	Details	Machining Time [s]	Tool Changing Time[s]	Setup Change [s]	Spindle repositioning Time [s]
	T0→T1		15		
	Setup L			60	
T1	L1	44			
	T1→T2		15		
	Setup R			60	
	Face→Slab Left				5
T2	R1	62			
	Slab Left→Slab Right				5
T2	R2	35			
	Slab Right→Face				5
T2	R3	212			
	T2→T3		15		
T3	R4	6			
	T3→T4		15		
	Setup B			60	
T4	B1	451			
	T4→T5		15		
T5	B2	15			
	T5→T2		15		
	Setup U			60	
T2	U1	789			
	Face→Tilted face				5
T2	U2	649			
T2	U3	76			
	Tilted Face→Lateral Tilted Face				5
T2	U4	350			
	Lateral Tilted Face→Face				5
T2	U5	28			
	T2→T6		15		
	Face→Tilted Face				5
T6	U6	108			
	T6→T7		15		
T7	U7	4			
	T7→T8		15		
	Tilted Face→Face				5
T8	U8	7			
	T8→T9		15		

T9	U9	2			
	T9→T10		15		
	Face→Tilted face				5
T10	U10	177			
	Tilted face→Face				5
T10	U11	79			
	T10→T11		15		
	Face→Tilted face				5
T11	U12	41			
	T11→T15		15		
	Tilted face→Face				5
T15	U13	1			
	T15→T12		15		
	Face→Tilted face				5
T12	U14	9			
	T12→T13		15		
T13	U15	8			
	T13→T14		15		
	Tilted face→Face				5
T14	U16	10			
	T14→T5		15		
T5	U17	107			
	Face→Tilted face				5
T5	U18	8			
	T16→T2		15		
	Setup FB			60	
	Tilted Face→Face				5
T2	FB1	27			
T2	FB2	27			
T2	FB3	105			
	T2→T16		15		
	Face→Left				5
T16	FB4	11			
T16	FB5	8			
	Left→Right				5
T16	FB6	4			
T16	FB7	6			
T10	FB8	74			
		3540	285	300	90
	TOT	4215	70		

In total, the time needed to produce the piece is **4215 s**, hence **70 minutes**, which are **1.167 hours**.

This indicates that the production time is **0.857 parts/hour**.

In production there have been **5 setup changes**, **19 tool changes** and **18 spindle repositions**.

From Fusion 360 we extracted these data:

	L	R	B	U	FB
Feed Distance (*m*)	1.000	20.518	10.652	58.499	5.342
Total Feed Time (*hh:mm:ss*)	00:00:44	00:04:33	00:07:28	00:39:39	00:04:08
Rapid Distance (*m*)	0.004	22.030	9.057	40.738	9.029
Total Rapid Time (*hh:mm:ss*)	00:00:00	00:00:44	00:00:18	00:01:21	00:00:18
Tool Changes	0	1	1	11	1
Total Tool Change Time (*hh:mm:ss*)	00:00:00	00:00:15	00:00:15	00:02:45	00:00:15
Total Machining Time (*hh:mm:ss*)	00:00:44	00:05:32	00:08:01	00:43:46	00:04:41

To those data we have to add the setup changes and the spindle repositions (we also considered the re-usage of some tools), hence arriving to the same results obtained before.

3.2 Detailed Informations on the Setups

All the 5 setups used the same fixture, but we needed to change the way the product was held by the clamps to ensure that the machine could operate without colliding with the equipment.

The **names** of the setups were given taking into account the main machined area.

The last setup, Front-Back, is named after the fact that we operated on both front and back faces of the piece.

The overall strategy involves clamping the piece along the X direction, ensuring that the excess stock makes vertical contact with the clamps on the fixture. This approach prevents the clamping process from damaging any previously machined surfaces.

- LEFT

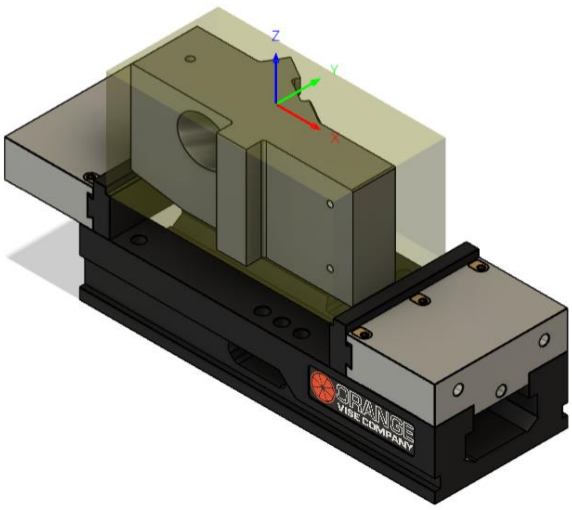

To machine the left surface of the piece, we clamped the stock along the X direction, as it had not been machined previously. Consequently, the opening corresponds to the X dimension of the stock, which is **260 mm**.

- RIGHT

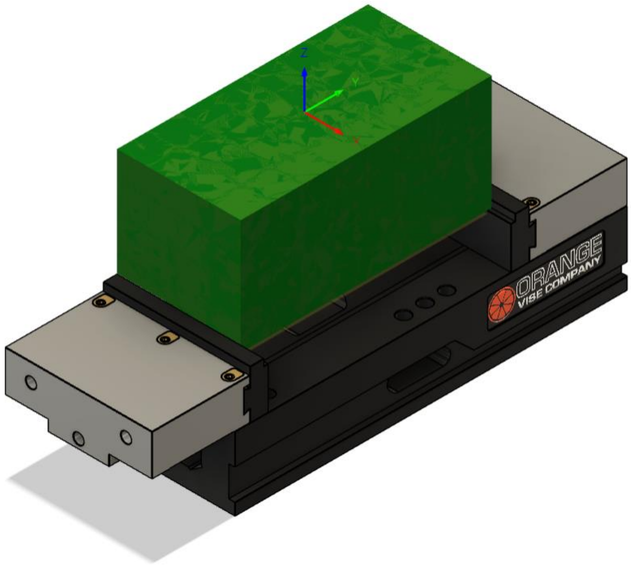

To machine the right surface of the piece, we re-clamped it along the X direction, maintaining an opening of **260 mm**. Unlike the previous setup, the contact area with the fixture now includes not only the stock but also the previously machined surface (from the bottom). However, since this surface does not have strict roughness requirements, clamping it posed no issues.

- BOTTOM

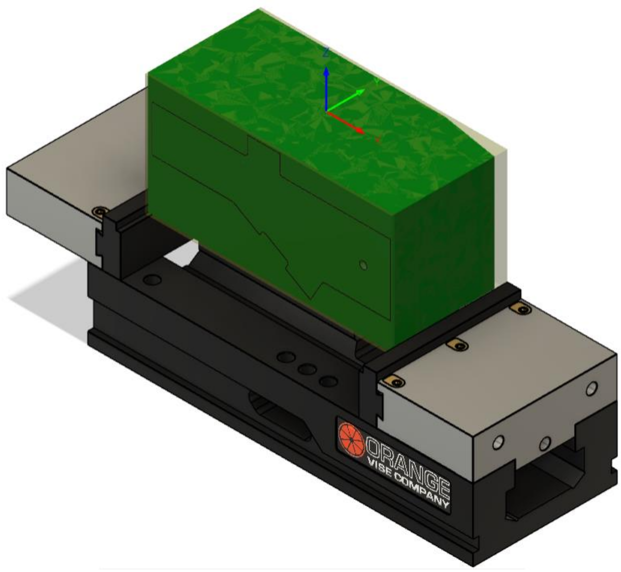

To machine the bottom surface of the piece, we re-clamped it along the X direction, maintaining the same **260 mm** opening. This time, the excess stock on the top surface of the piece was placed in contact with the fixture from below, ensuring that no machined surfaces came into contact with the fixture.

- TOP

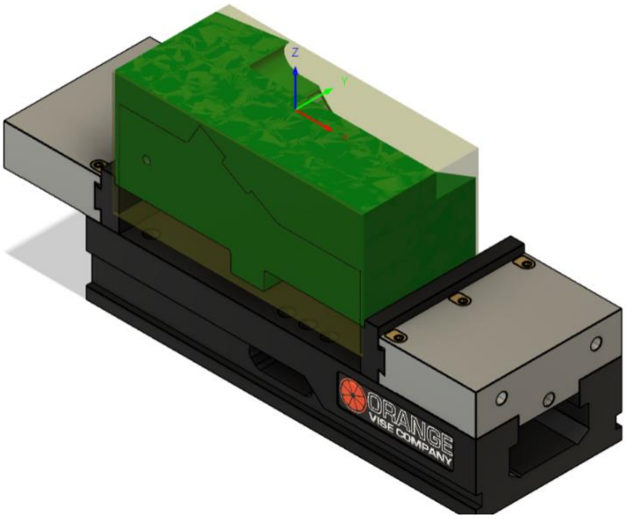

To machine the top surface of the piece, we reversed the fixturing from the previous setup, again clamping it along the X direction with a **260 mm** opening. The previously machined bottom surface, which does not have strict roughness requirements, was placed in contact with the fixture from below, allowing for secure clamping without any issues.

- FRONT-BACK

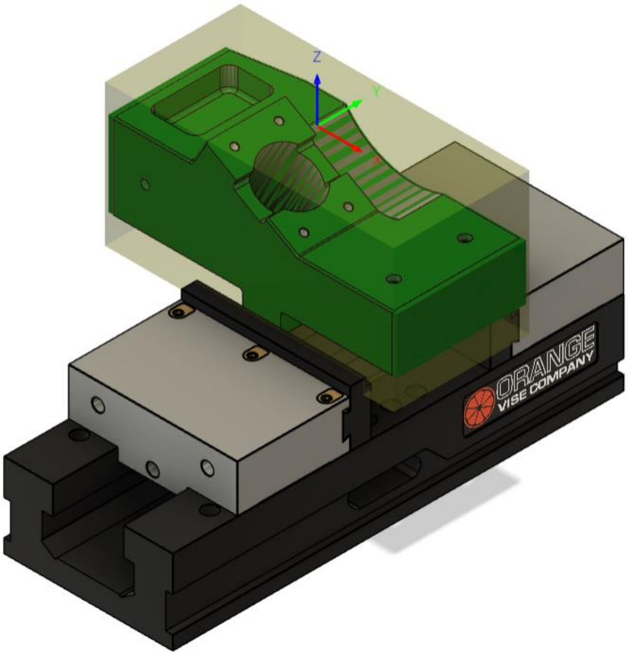

The clamping strategy was adjusted to machine the front and back surfaces, which had been clamped in the other setups. This new approach involved securing the lateral surfaces of the piece from the sides and the bottom surface from below. Specifically, the bottom of the T-shaped part of the piece was clamped, resulting in an opening of **116 mm**. This setup was feasible because the surfaces in contact with the fixture did not have strict tolerance requirements, ensuring that the quality of the piece was not compromised.

3.2.1 Sequenced operations and Process parameters

In this section there is a detailed description of each operation performed in each setup with also the chosen process parameters. For operations performed in multiple passes, the tables show the total axial/radial depth of cut, while the per-pass depths are detailed in the text description.

- LEFT

In this setup, only one operation was performed: the face milling of the left face of the piece (**L1**). We selected a large face mill to cover the entire surface in a single pass. Hower due to power limitation issues we decided to cover the surface in 2 passes, as not to exceed the spindle power limit.

The surface to be machined measured 260 x 128 mm, so we opted for a face mill with a diameter larger than the width of the surface, specifically 160 mm. Additionally, we chose a face mill with a differential pitch design to enhance the stability of the setup during the operation.

Since this operation did not have strict requirements for surface roughness, the use of a differential pitch face mill was ideal. This design minimized vibrations while achieving the desired surface finish. (#PA indicates the number of passes). The radial depth of cut for each pass is $a_e = 75\ mm$.

Tool	**Code**	$v_c\ \left({}^{m}/_{min}\right)$	$f_z\ \left({}^{mm}/_{tooth}\right)$	**DC** (mm)	$a_e\ (mm)$	$a_p(mm)$	$K_r\ (°)$	**#PA**
T1	**L1**	245	0.25	160	128	3	45	2

- RIGHT

In this setup, we carried out four operations. The first two operations focused on slab milling the right surface (**R1** and **R2**), the third was again a slab milling operation to produce the curved surface (**R3**), while the final operation involved drilling a deep through hole (**R4**).

For the first two operations, the objective was to remove material from the left surface. However, due to a shifted surface, a standard face milling operation was insufficient. As a result, we opted for slab milling to accommodate the shift in the surface. Since no tool with a flute length long enough to cover the full surface (128mm) was available, we selected the longest tool possible (100mm) and performed two passes, one from the right and one from the left. However, we observed that each of the two slab milling operations exceeded the power limits. As a result, we decided to perform multiple passes with an axial depth of cut $a_p = 9.7\ mm$ per pass.

The third operation aimed to produce the curved surface. This was performed in the current setup to comply with the constraints of the 4-axis machine. While similar to the previous two operations, the substantial amount of material to be removed necessitated multiple passes with an axial depth of cut set to 4.5 mm. This approach ensured that the spindle power limitations were not exceeded.

Finally, we executed a drilling operation on the right surface to create the deep through hole.

Tool	Code	$v_c\ (m/min)$	$f_z\ (mm/tooth)$	DC (mm)	$a_e\ (mm)$	$a_p(mm)$	$K_r\ (°)$
T2	**R1**	240	0.375	25	3	99.51	90
T2	**R2**	240	0.375	25	3	58.03	90
T2	**R3**	240	0.375	25	25	58.03	90

Tool	Code	$v_c\ (m/min)$	$f\ (mm/rev)$	DC (mm)	h (mm)	$\varepsilon\ (°)$
T3	**R4**	100	0.3	8	110.33	118

- BOTTOM

In this setup, we executed two distinct operations, each designed to optimize both machining efficiency and the quality of the final part. The first operation was pocketing, which enabled the creation of the bottom surface of the piece from the stock material (**B1**).

This operation was critical for achieving the necessary depth and flatness of the surface. In selecting the tool for this process, we sought to balance surface finish requirements, specifically the adherence to the given roughness specifications, with operational feasibility. We opted for a flat end mill with a flute length slightly exceeding the depth of the cut. This choice allowed for greater stability and material removal efficiency while still maintaining the desired surface finish. The diameter of this flat end mill was deliberately smaller than that of the T2 tool, offering improved maneuverability in confined geometries and ensuring the precise material removal needed for pocketing. Since we had power limitation issues we decided to perform this operation in multiple passes, each one with a depth of cut of 9.2 mm, in order not to exceed the 16 kW spindle power limit.

The second operation involved performing fillets around the T-shaped part of the piece (**B2**).

To achieve the desired radius of the fillets, a ball end mill with a 3 mm radius was employed, corresponding directly to the required fillet radius. The decision to use a ball end mill was driven by its ability to produce smooth, continuous curves that are essential for such geometries. Importantly, the height of the ball end mill was sufficient to clear any previously machined surfaces, preventing potential collisions while ensuring uninterrupted toolpath progression.

Tool	Code	$v_c\ (m/min)$	$f_z\ (mm/tooth)$	DC (mm)	$a_e\ (mm)$	$a_p(mm)$	$K_r\ (°)$
T4	**B1**	200	0.185	20	20	25	45
T5	**B2**	220	0.08	6	3	20	45

- TOP

In this setup, we performed 18 operations. The first 9 were focused on roughing or creating surfaces with high roughness requirements, while the remaining 9 were dedicated to finishing.

The initial operation involved creating the entire top surface (**U1**), making multiple passes, each one of 4.5 mm of depth, for the same reason stated before for the **R3** operation.

Subsequently, we machined the top tilted surface (**U2**), the slots (**U3**), the right surface of the tilted face (**U4**), and performed the roughing of the pocket (**U5**). For these operations, we continued using the same tool to minimize tool changes. Moreover we again considered multiple passes of 4.5 mm of depth for those operations (not for the **U3** operation) for respecting power limits.

The last four roughing operations were dedicated to the holes. First, we pre-drilled the large through hole (**U6**) with a 51 mm drill, leaving stock for finishing. Then, we pre-drilled the blind holes on the tilted surface (**U7**) using a 6 mm drill, preparing them for tapping. Similarly, we pre-drilled the through holes on the top surface (**U8**) with a 6.8 mm drill, also for tapping. Finally, we rough-machined the counterbore holes on these through holes (**U9**) using a 9.8 mm drill, creating space for the reaming operation.

Tool	Code	$v_c\ (m/min)$	$f_z\ (mm/tooth)$	DC (mm)	$a_e\ (mm)$	$a_p(mm)$	K_r (°)
T2	**U1**	240	0.375	25	25	53	45
T2	**U2**	240	0.375	25	25	53.90	45
T2	**U3**	240	0.375	25	10	8	45
T2	**U4**	240	0.375	25	15	12.5	45
T2	**U5**	240	0.375	25	25	20	45

Tool	Code	$v_c\ (m/min)$	$f(mm/rev)$	DC (mm)	h (mm)	ε (°)
T6	**U6**	141.21	0.0787	51	107.387	180
T7	**U7**	170	0.18	6	12	147
T8	**U8**	110	0.23	6.8	50	140
T9	**U9**	85	0.27	9.8	5	140

The first finishing operation focused on the tilted surface (**U10**), where we used a small-diameter flat end mill to achieve the desired surface roughness and ensure greater accuracy. The same tool (T10) was then utilized for finishing the pocket (**U11**), addressing both the bottom surface and the removal of excess stock from the pocket's contour. This tool was chosen because its smaller radius was suitable for the curved lines of the pocket, which had a radius of 8 mm. Here we performed multiple passes of 16.2 mm of depth, since doing it in one pass was unfeasible in terms of power.

Next, we moved on to finishing the holes. The first operation was the finishing of the large through hole (**U12**), performed using a boring tool. A boring operation was selected because no reamer with a 52 mm diameter was available in the catalogs we consulted.

Following that, we finished the counterbore holes (**U13**) using a 10 mm reamer to meet the required tolerance level. For the countersinking of the blind holes (**U14**), we used an 8 mm drill with a 90° tip angle, as specified in the design.

We then tapped the blind holes (**U15**) using a tap drill to achieve the M7x1 thread specification. This operation required a pre-drilled 6 mm hole, which had been created earlier during the **U7** operation. We used a tap drill with spiral flutes to guarantee the chip flow out of the blind holes.

Finally, we performed tapping on the through holes on the top surface (**U16**). Here, we used a tap drill to achieve the M8x1.25 thread specification. This required a pre-drilled 6.8 mm hole, created previously in the **U8** operation. We used a tap drill with spiral point to push the chip forward in the through holes.

Tool	**Code**	$v_c\ (m/min)$	$f_z\ (mm/tooth)$	**DC** (mm)	$a_e\ (mm)$	$a_p(mm)$	K_r (°)
T10	**U10**	205	0.07	6	3.6	0.2	45
T10	**U11**	205	0.07	6	3.6	17	45

Tool	**Code**	$v_c\ (m/min)$	$f\ (mm/rev)$	**DC** (mm)	**h** (mm)	ε (°)
T11	**U12**	251	0.0928	52	107.387	//
T15	**U13**	180	0.8	10	5	//
T12	**U14**	70.1	0.07874	7	0.682	90
T13	**U15**	27	1	M7x1	12	//
T14	**U16**	27	1.25	M8x1.25	45	//

The final two operations were dedicated to filleting.

The first of the last two operations involved creating fillets on the entire top surface (**U17**), while the second targeted the slots on the tilted surface (**U18**). Both operations were completed using the same tool (T5) that was previously used for filleting in the bottom setup.

Tool	**Code**	$v_c\ (m/min)$	$f_z\ (mm/tooth)$	**DC** (mm)	$a_e\ (mm)$	$a_p(mm)$	K_r (°)
T5	**U17**	220	0.08	6	3	3	45
T5	**U18**	220	0.08	6	3	8	45

- FRONT-BACK

In this setup, we performed eight operations: three slab milling operations to produce the front surface, the back surface and to produce the back surface corner chamfers, followed by five chamfering operations.

The first slab milling operation was conducted on the front surface (**FB1**), and the second on the back surface (**FB2**). Both operations utilized the same tool as the **R3** operation, in multiple passes with axial depth of cut of 9.7 mm for power limitation reasons.

The third slab milling operation was performed on the back corner (**FB3**). It can be seen as a specialized chamfering technique. Instead of using a standard chamfering tool, we employed the same tool used for the **U1** operation, essentially performing side milling to create the chamfer. This approach was necessary because the left side of the back surface was inclined at an angle that was not 90°, making it impossible to use the standard chamfering tool without leaving residual stock. We performed multiple passes with axial depth of cut of 12.2 mm.

The last five operations were chamfering. The first chamfering operation was applied to the left side of the piece (**FB4**), the second targeted the edges of the left tilted surface (**FB5**), while the third was applied on the right surface of the piece (**FB6**) and the fourth targeted the edges of the right curved surface (**FB7**).

The last chamfering operation was performed on the whole contour of the top surface (**FB8**).

For these chamfering tasks, we used a chamfer mill with a 45° tip angle and a 4 mm flute length (T16). This tool was selected because the chamfers required were 1.5 mm long with a 45° angle, making it a precise match for the design specifications.

We decided to perform all those chamfering tasks in this setup to respect the constraint of the 4 axes machine.

Tool	**Code**	$v_c\ (m/min)$	$f_z\ (mm/tooth)$	**DC** (mm)	$a_e\ (mm)$	$a_p(mm)$	K_r (°)
T2	**FB1**	240	0.375	25	3	50	90
T2	**FB2**	240	0.375	25	3	76	90
T2	**FB3**	240	0.375	25	1.5	76	90
T16	**FB4**	220	0.07	14	1.5	1.5	90
T16	**FB5**	220	0.07	14	1.5	1.5	90
T16	**FB6**	220	0.07	14	1.5	1.5	90
T16	**FB7**	220	0.07	14	1.5	1.5	90
T16	**FB8**	220	0.07	14	1.5	1.5	45

3.3 Manufacturing Resources

Tool #	**Chosen Tool**	**Chosen Insert**	**z**	**Catalogue**	**Tool Link**	**Insert Link**
T1	CoroMill® 745 face milling cutter (745-160Q40-21MD)	CoroMill® 745 insert for milling (745R-2109E-M50 4230)	10	Sandvik Rotating Tools	T1	Insert T1
T2	CoroMill® Plura solid carbide end mill for High Feed Side milling (2P370-2500-PB 1740)		4	Sandvik Solid Round Tools	T2	

T3	Mitsubishi MVS (MVS0800X20S080)		2	Mitsubishi Materials Cutting Tools		
T4	CoroMill® Plura solid carbide end mill for heavy roughing (1P222-2000-XB 1630)		4	Sandvik Solid Round Tools	T4	
T5	CoroMill® Plura solid carbide ball nose end mill for profiling (R216.54-06040RAL40G 1620)		4	Sandvik Solid Round Tools	T5	
T6	Mitsubishi MVX (MVX5100X4F50)	UM Chip Insert (SOMX166508-UM)	2	Mitsubishi Materials Cutting Tools		
T7	CoroDrill® 860 solid carbide drill (860.1-0600-037A1-PM P1BM)		6	Sandvik Solid Round Tools	T7	
T8	Mitsubishi MVS (MVS0680X10S070)		2	Mitsubishi Materials Cutting Tools		
T9	Mitsubishi MVE (MVE0980X03S100)		2	Mitsubishi Materials Cutting Tools		
T10	CoroMill® Plura solid carbide end mill for finishing (R215.36-06050-AC13L 1620)		6	Sandvik Solid Round Tools	T10	
T11	CoroBore® 825 fine boring tool (825-56TC09-C5)	CoroTurn® 107 insert for turning (TCMT 09 02 04-MF 1125)	1	Sandvik Rotating Tools	T11	Insert T11
T12	Mitsubishi DLE (DLE0700S070P090)		2	Mitsubishi Materials Cutting Tools		

T13	CoroTap™ 300 cutting tap with spiral flutes (T300-XM100DA-M7 C110)		3	Sandvik Solid Round Tools	T13	
T14	CoroTap™ 200 cutting tap with spiral point (T200-XM100DA-M8 C110)		3	Sandvik Solid Round Tools	T14	
T15	CoroReamer™ 835 solid carbide reamer (835.B-1000-A1-PF 1024)		10	Sandvik Solid Round Tools	T15	
T16	CoroMill® Plura solid carbide end mill for chamfer milling (1U000-0600-400-XA 1620)		4	Sandvik Solid Round Tools	T16	

The fixture used was the one seen during Lab Classes from Orange Vise Company.

For a scaling comparison, the side of the clamp shown in figure measures 151.70 mm.

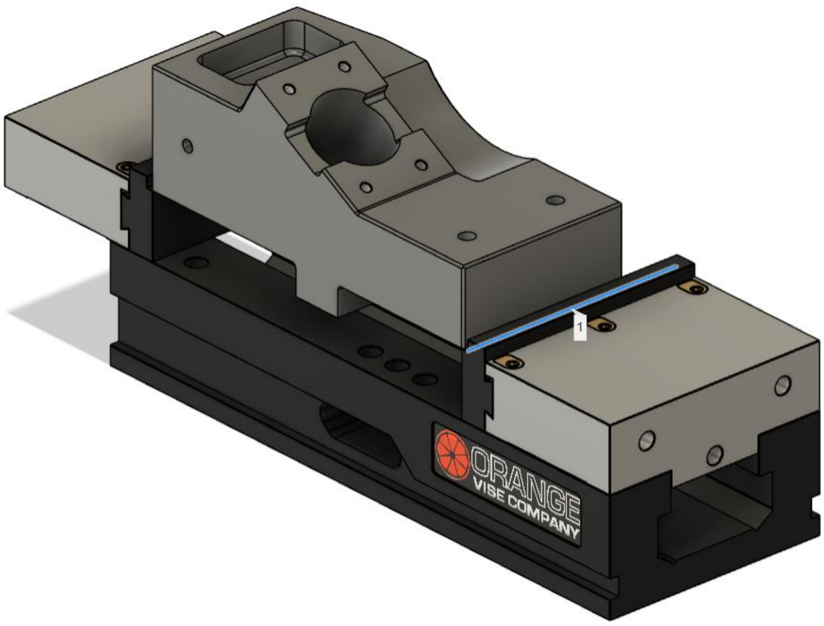

4) Verification of operations

4.1 Power and spindle rotational speed verification

Using the formula presented in the first paragraph, we can verify that the power, spindle speed, surface roughness, and compliance with Shmaltz's equation for all operations, along with their respective tools, adhere to the following constraints:

- Maximum Spindle Power: **16 kW**
- Maximum Spindle Rotational Speed: **14000 rpm**
- $\boldsymbol{R_a \leq 3.2\ \mu m}$ for operations **U10**, **U11**, **U12**, **U13**, $\boldsymbol{R_a \leq 12.5\ \mu m}$ for the others

Operation Code	Tool #	Pc [kW]	n [RPM]	R_a [μm]	Schmaltz's Equation
L1	T1	15.097	487	0.1860	✓
R1	T2	15.881	3056	0.3516	✓
R2	T2	15.881	3056	0.3516	✓
R3	T2	15.697	3056	0.3516	✓
R4	T3	1.926	3979	H10	✓
B1	T4	15.742	3183	0.1095	✓
B2	T5	13.017	11671	0.0667	✓
U1	T2	15.697	3056	0.3516	✓
U2	T2	15.697	3056	0.3516	✓
U3	T2	5.412	3056	0.3516	✓
U4	T2	15.697	3056	0.3516	✓
U5	T2	15.697	3056	0.3516	✓
U6	T6	6.212	875	H10	✓
U7	T7	1.666	9019	H10	✓
U8	T8	1.482	5151	H10	✓
U9	T9	1.850	2762	H10	✓
U10	T10	0.152	10876	0.0510	✓
U11	T10	15.959	10876	0.0510	✓
U12	T11	1.076	1536	0.6781	✓
U13	T15	0.521	5730	H7	✓
U14	T12	0.465	3188	H7	✓
U15	T13	0.464	1228	M7x1	✓
U16	T14	0.693	1074	M8x1.25	✓
U17	T5	1.953	11671	0.0667	✓
U18	T5	5.207	11671	0.0667	✓
FB1	T2	15.881	3056	0.3516	✓
FB2	T2	15.881	3056	0.3516	✓

FB3	T2	15.788	3056	0.3516	✓
FB4	T16	0.883	5002	0.0170	✓
FB5	T16	0.883	5002	0.0170	✓
FB6	T16	0.883	5002	0.0170	✓
FB7	T16	0.883	5002	0.0170	✓
FB8	T16	0.681	5002	0.0170	✓

In conclusion, we can confirm that all operations are feasible, as neither the power requirements nor the spindle speeds exceed the specified limits.

Additionally, the Fusion360 simulations for each setup further validate the feasibility of the operations, as the product color remains within the acceptable range and no collision warnings are displayed in the simulation info window.

4.2 Step by step verification formulas

4.2.1 Face Milling Operations

- **Operations: L1, U10**

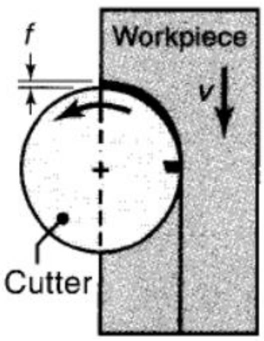

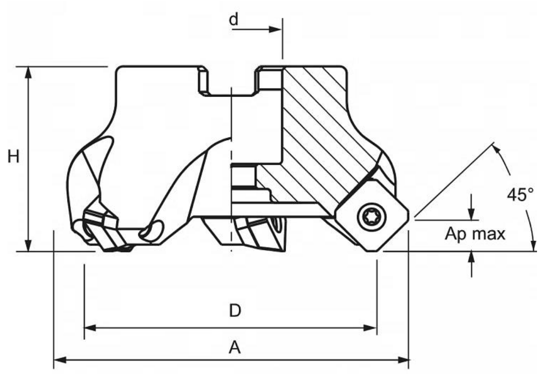

As first thing it is needed to compute the number of working teeth:

$$\varphi = \arcsin\left(\frac{\frac{D}{2} - a_e}{\frac{D}{2}}\right); \ \varphi_0 = \frac{2\pi}{Z}$$

$$z = \frac{\varphi}{\varphi_0}$$

Now we need to compute the cutting force:

$$h_D = f_z * \cos(\theta) * \sin(k_r)$$

$$A_D = h_d * a_p$$

$$k_c = \frac{k_{cs}}{{h_d}^x}$$

$$F_c = k_c * A_D$$

Now we compute the cutting torque:

$$T_c = \sum_{i=1}^{z} \frac{Fc * \frac{DC}{2}}{1000}$$

In the end we compute the cutting power:

$$n = \frac{v_c * 1000}{\pi * DC}$$

$$\omega = \frac{2\pi n}{60}$$

$$P_c = T_c * \omega$$

The results are in the table above.

For the roughness, we need to guarantee a roughing quality of $R_a = 3.2\ \mu m$ for the **U10** operation and $R_a = 12.5\ \mu m$ for the other. In order to compute it, we have to apply these formulas:

$$R_a = \frac{{f_Z}^2 * 1000}{32 * r}$$

We had to be careful about the value of r, since if we worked with a tool with inserts we had to take the radius of the considered insert, otherwise we took the radius of the tool. For example, for our considered insert for the tool T1, the cutting radius is 10.5 mm.

Moreover we need to verify that the Shmaltz's equation is respected:

$$\frac{f_Z}{2} < min(r * \sin(k_r);\ r * \sin(k_r'))$$

4.2.2 Slab Milling Operations

- **Operations: R1, R2, R3, FB1, FB2, FB3**

For slab milling operations we adopted the same formulas as face milling, but considering an entering angle of 90 degrees and considering that:

$$h_D = f_z * \sin(\theta)$$

In these operations the quantity of removed material is often huge, hence we often performed multiple passes.

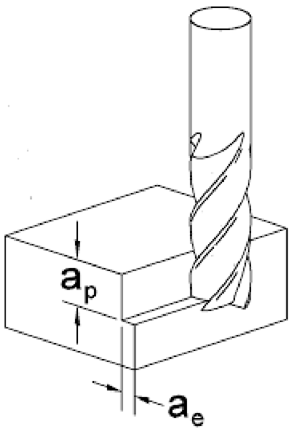

4.2.3 Pocketing Operations

- **Operations: B1**, **U1**, **U2**, **U3**, **U4**, **U5**, **U11**

The pocketing operation is one of the most demanding and power-intensive processes, as it is typically performed in scenarios involving the removal of a significant amount of material.

When it was required to achieve higher surface quality we divided the operation in 2 steps, a roughing one and a finishing one, in order to reach the desired roughness.

Since this operation was often performed in multiple passes, it could be viewed as multiple stages of face milling, simplifying both the modeling process and the computations. While pocketing and face milling are fundamentally different operations, pocketing involves creating recessed areas with defined boundaries and depths, whereas face milling focuses on flattening surfaces, they can share similarities under certain conditions. Specifically, when pocketing is performed with wide, shallow passes over a flat area, it can resemble face milling in terms of tool paths and material removal. Therefore, for the purpose of simplification in modeling and calculations, the pocketing operation in this case was treated as analogous to face milling.

However, in the operations **U5** and **U11**, this type of modeling is not applicable because we were producing an actual pocket with defined boundaries and depth on a pre-machined surface. Unlike face milling, which primarily involves removing material uniformly across a flat area, pocketing in these cases requires precise tool paths to shape the pocket's vertical walls, corners, and bottom surface. This level of geometric complexity and the need to follow the pocket's specific contours mean that the operation does not resemble face milling at all, as it goes beyond simply flattening a surface.

Hence, in order to model the **U5** and **U11** operations we use a two-step approach: an initial **drilling phase** for entry and a **face milling phase** for horizontal material removal. This approach balances computational simplicity with accuracy in representing the key aspects of the operation.

- ***Drilling Phase***

The drilling phase models the tool's entry into the material, accounting for axial material removal. Although a flat-end mill is used, this phase can be approximated using formulas for drilling operations, as the tool primarily engages in the axial direction during the initial plunge. The cutting torque (T_c) and power (P_c) are computed as:

$$F_C = k_c * A_d; A_d = a_p * DC$$

$$T_c = \frac{F_c * \frac{D}{2}}{1000}; \ \omega = \frac{2\pi n}{60}$$

$$P_c = T_c * \omega$$

- ***Face Milling Phase***

After the initial plunge, the operation transitions to material removal in the horizontal plane, modeled as face milling with a 90° entering angle. This step simplifies the pocketing operation by treating it as multiple stages of flat-bottom milling. The cutting power (P_c) for this phase is calculated using:

$$h_D = f_z * \cos(\theta) * \sin(k_r)\,;\; A_D = h_d * a_p$$

$$F_c = k_c * A_D$$

$$P_c = \frac{F_c * v_c}{60 * 1000}$$

The power to consider for the entire operation is the higher of the two values, as the operations are performed at different times. Therefore, it is:

$$P_c = \max\left(P_{c_{drilling\ phase}}, P_{c_{face\ milling\ phase}}\right)$$

In both cases the highest one was the one of the face milling phase.

4.2.4 Filleting operations

- **Operations: B2, U17, U18**

The filleting operation can be conceptualized as a side milling operation, where the tool engages the material along the side rather than on the face. However, in filleting, the portion of material being cut away is typically much smaller compared to traditional side milling. Despite this difference, the cutting mechanics remain similar to those of slab milling, as the tool still removes material primarily along its side.

In both slab milling and filleting operations, the cutting force is influenced by the depth of cut and the material being machined. Since the material removal rate in filleting is small, the cutting forces and power requirements are generally lower than in larger side milling operations. Because of this similarity in the cutting process, the same formulas and principles used in slab milling, which involve parameters like depth of cut and radial engagement, can also be applied to filleting.

By using these established formulas, it becomes easier to estimate the cutting forces and power consumption in filleting, ensuring that the machining operation is properly optimized.

4.2.5 Chamfer milling operations

- **Operations: FB4, FB5, FB6, FB7, FB8**

Chamfer operations remove minimal material, so they are expected to be feasible. However, we can also model them as a specific case of face milling. The tool has a tip diameter of 6 mm, and the external working diameter can be determined from the chamfer geometry, yielding $D_{ext} = 12\ mm$. The tool's torque is applied at the center of the working area:

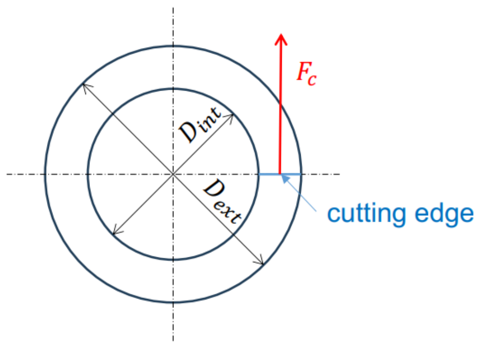

$$T_{c,max} = z * F_{c,max} * \frac{\frac{\frac{DC_{ext}}{2} + \frac{DC_{int}}{2}}{2}}{1000}$$

The other formulas are the same seen in face milling.

4.2.6 Drilling operations

- **Operations: R4, U6, U7, U8, U9**

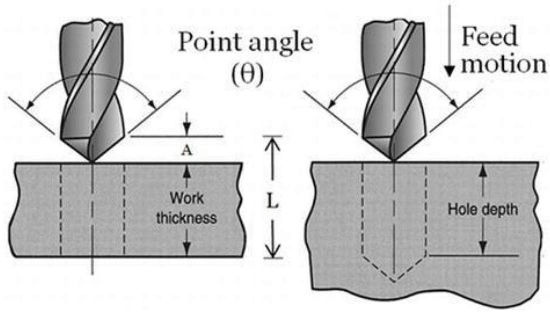

In order to compute the cutting power for drilling we firstly have to compute the chip thickness:

$$h_D = \frac{f}{2} * \sin\left(\frac{\theta}{2}\right)$$

Then we compute the cutting force:

$$A_D = \frac{f}{2} * \frac{DC}{2}$$

$$F_c = k_c * A_D$$

Then we computed the power:

$$T_c = \frac{F_c * \frac{DC}{2}}{1000}$$

$$n = \frac{v_c * 1000}{\pi * DC}$$

$$\omega = 2\pi * \frac{n}{60}$$

$$P_c = T_c * \omega$$

4.2.7 Reaming operations

- **Operations: U13**

The formulas for reaming operations are the same as drilling, but with 2 exceptions:

$$A_D = f_z * \frac{(DC_{ext} - DC_{int})}{2}$$

$$T_c = \frac{Z * F_c * \frac{DC_{ext} + DC_{int}}{4}}{1000}$$

4.2.8 Tapping operations

- **Operations: U15, U16**

The formulas used for tapping are the same as reaming, but we consider the considered pitch as the feed:

$$f = Thread\ Pitch$$

4.2.9 Countersinking operations

- **Operations: U14**

This operation can be modeled in two ways, depending on the considered tool:

- ***Standard Drilling***

We could model this operation as a drilling one, but with a low depth of cut and point angle of 90°.

- ***Chamfer Milling Operation***

We could model this operation as a chamfer milling operation over a drilled hole, where all the cutting edges are working.

We chose to model the operation as a drilling one.

4.2.10 Boring operations

- **Operations: U12**

This particular operation is meant for finishing some pre-drilled holes. It can be compared to a turning operation, because of the **similarities** in the cutting mechanics and tool geometry. Both processes use single-point cutting tools (or similar tools) that remove material through radial and axial movements. As a result, many of the same cutting principles, such as chip thickness, cutting force, and power, apply to both turning and boring, which is why turning formulas can be directly adapted for use in boring.

Therefore we have that the cutting force is:

$$a_p = \frac{DC_{final} - DC_{initial}}{2}$$

$$A_D = a_p * f$$

$$F_c = k_c * A_D$$

Hence the cutting power is:

$$P_c = \frac{F_c * v_c}{60 * 1000}$$

Of course, we apply the same formulas for computing the roughness.

5) Discussion

- ***Tolerance***

Taking into consideration the hole tolerance requirement H10 or H7 we pursued two different actions:

- For H10 holes (general requirement) we only needed one drilling operation.
- For H7 holes (high requirement) we first needed a drilling operation and then a reaming/boring operation.

For the threaded holes we first needed a drilling operation and then a tapping operation.

We called “pre-drilling” every operation that needed further reaming/threading to ensure the tolerance requirement.

The setups and operations order mattered, since in this way we were able to guarantee all the parallelism specifications, mainly with the A surface. We were also able to guarantee the perpendicularity of F with respect to the D surface, since we worked out these parts in the same setup following a correct operation order, like we were able to guarantee the angularity specification of the D surface with respect to the A one. The other specifications were also respected for the same reasons explained above.

- ***Roughness***

For the roughness requirements, we follow a similar reasoning:

- We can find a general requirement of Ra 12.5, and a high requirement of Ra 3.2.
- When needed a high requirement, we divided the machining into a roughing operation and a finishing operation.
- For the roughing operation we just needed to be sure to have a *stock to leave*, while for the finishing we needed to verify that our Ra value stayed below the goal Ra. For holes roughing, we just drilled using a tool with lower diameter with respect to the desired hole diameter.
- Moreover, we verified that the Schmaltz inequality was verified, so that the feed did not exceeded the limit.

- ***Tool Selection***

In order to choose the correct tool for each operation we used the Sandvik and the Mitsubishi catalogs. We chose the feed and the cutting velocity values by looking at the tool tables, hence basing our choices on the material to cut and on the cutting conditions. However, our material P.1.4.Z.AN was often not included in the tables, therefore we had to take the parameters of a similar unalloyed steel material in terms of hardness calculated in HB.

- ***Setup Choices***

We decided to use the considered setups and in that order not only to guarantee the specifications, but also for not ruining the surfaces during the operations, as already described in chapter 3.2.

- ***Chamfers Imperfections***

Another minor yet important consideration to make is that the chamfer of the top surface has some imperfections for the change in the angle of the top tilted surface. The chamfer is a very minor operation also in terms of size, so we neglected this imperfection.

- ***Challenges***

In conclusion, this project really challenged our technical abilities and the ability to work as a team, designing together the process and then splitting the tasks for each member.

In particular, we had to go through different process iterations because we progressively found more and more constraints and problems to solve, showing an increasing awareness of the entire project and of the workflow.